journal

J. Am. Ceram. Soc., 90 [12] 3852–3858 (2007)
DOI: 10.1111/j.1551-2916.2007.01997.x

Rapid Synthesis of Ferromagnetic $La_{1-x}Na_xMnO_3$ ($0.00 \leq x \leq 0.25$) by the Solution Combustion Method

Chikkadasappa Shivakumara,[†,‡] Manjunath B. Bellakki,[‡] Annigere S. Prakash,[§] and Nagsampagi Y. Vasanthacharya[‡]

[‡]Solid State and Structural Chemistry Unit, Indian Institute of Science, Bangalore 560 012, India

[§]Functional Materials Division, Central Electrochemical Research Institute, Karaikudi 630 006, Tamil Nadu, India

Rapid synthesis of sodium-substituted lanthanum manganite phases is reported by the solution combustion method using oxalyl dihydrazide (ODH), as fuel. As-synthesized compounds are amorphous in nature; crystallinity was observed on heating at 800°C for 5 min. Structural parameters were determined by the Rietveld refinement method using powder X-ray diffraction data. Parent $LaMnO_3$ compound crystallizes in the orthorhombic structure (space group *Pbnm* No. 62). Sodium-substituted compounds crystallize with rhombohedral symmetry (space group *R*-3*c*, No.167). On increasing the sodium content, unit cell volume decreases and Mn–O–Mn bond angle increases. The fourier transform infrared spectrum shows two absorption bands around 600 and 400 cm^{-1} for the compositions $x = 0.0$, 0.05, and 0.10. Mn^{3+}/Mn^{4+} ratio was determined by iodometric titration. Electrical resistivity measurements reveal a composition-controlled metal to insulator transition (T_{M-I}), the maximum T_{M-I} was observed for the composition $La_{0.85}Na_{0.15}MnO_3$ at 285 K. Increase in magnetic moment is observed with increase in crystallite size. Room temperature vibrating sample magnetometer data indicate that for the composition up to $x = 0.10$, the compounds are paramagnetic whereas composition with $x = 0.15$, 0.20, and 0.25 show magnetic moments 34, 39, and 33 emu/g, respectively.

I. Introduction

DIVALENT metal ions (Ca^{2+}, Sr^{2+}, Ba^{2+}, and Pb^{2+}) substitution for La^{3+} ion in $LaMnO_3$ inducing ferromagnetic metallic property has been known for a long time.[1] Observation of colossal magnetoresistance (CMR) in $La_{1-x}Ba_xMnO_3$ thin films has created new interest in these materials.[2] New phenomena, viz. charge, spin, and orbital ordering, have been discovered in these perovskite-based rare-earth manganites as can be read from a recent review.[3] Monovalent ion-doped rare earth manganites of the general formula $Ln_{1x}A_xMnO_3$ (Ln = La, Pr, Nd; A = Na, K, Rb) provide another series of new oxides to study the physical phenomena of insulator-to-metal transition and CMR.[4–9] Alkali metal ion-doped lanthanum manganites have been prepared by ceramic methods,[4,5] alkali-flux method,[6,9] fused salt electrolysis.[10]

The ratio of Mn^{3+}/Mn^{4+} is an important factor in insulator to metal (I–M), transition and magnetic phase transition in manganites. Generally, divalent ions (Ca, Sr, Ba, and Pb)-doped compounds exhibit composition-controlled I–M transition. It is possible to achieve an equal amount of hole doping with half the number of the monovalent ions, because for the same amount of aliovalent dopant, the hole density is twice that of divalent ion doping.

The solution combustion method offers an advantage over other conventional methods. It is a low-temperature-initiated exothermic and self-propagating process. Patil *et al.*[11] have reviewed the synthesis of various oxide materials by the combustion reactions of redox mixtures containing stoichiometric amounts of respective metal nitrates (oxidizers) and fuels such as urea, hydrozides (Carbohydrazide, CH), oxalydihydrazide (ODH), malonic acid dihydrazide (MDH), tetraformaltrisazine (TFTA), and glycine. Using the solution combustion method, a wide range of technologically useful oxides were prepared, having magnetic, dielectric, electrical, mechanical, luminescent, and optical properties. Bera *et al.* synthesized new redox catalysts of Ag/CeO_2[12] and Cu/CeO_2.[13] This method was also applied to prepare divalent ion-doped-lanthanum manganites.[14] Recently, nanocrystalline $La_{1-x}Ba_xMnO_3$,[15] $La_{1-x}Sr_xMnO_3$,[16] and sodium-doped lanthanum manganites were prepared by the sol–gel and propellant method.[17] In the present study we have synthesized series of ferromagnetic sodium-doped lanthanum manganates by the solution combustion method at relatively low temperatures using ODH as a fuel and studied the structural, transport, and magnetic properties.

II. Experimental Procedure

The title compounds were prepared by the solution combustion method using ODH as a fuel. The detailed procedure for calculating the metal nitrates to fuel ratio has been described elsewhere.[11,18] Stoichiometric amounts of $La(NO_3)_3$ (obtained by dissolving the requisite amount of preheated La_2O_3 at 800°C), $NaNO_3$, and $Mn(NO_3)_2 \cdot 4H_2O$ were dissolved in a minimum amount of water in a pyrex dish. Calculated amounts of the fuel ODH were added. The ODH dissolved and formed a clear solution, which was introduced into a muffle furnace preheated to 400°C. The mixture boiled, followed by frothing and ignited with evolution of a large amount of gases. The flame persisted for about a minute leaving behind a residual black colored fine powder. Assuming complete combustion, the general equation for the formation of samples can be proposed as follows:

$$(1-x)La(NO_3)_3(aq) + xNa(NO_3)(aq) + Mn(NO_3)_2(aq) + C_2H_6N_4O_2(aq) \rightarrow La_{1-x}Na_xMnO_3(S) + CO_2(g) + H_2O(g) + N_2(g)$$

All the samples were characterized by powder X-ray diffraction (XRD) using a Philips (the Netherlands) X'pert Pro diffractometer with Cu$K\alpha$ ($\lambda = 1.5418$ Å) using a graphite monochromator to filter the K_β lines. For Rietveld refinement, data were collected at a scan rate of 1°/min with a 0.02° step size for 2θ from 10° to 80°. The data were refined using the FullProf Suite-2000 version. Morphology and compositional analysis were carried out in a scanning electron microscope (SEM) fitted with an energy dispersive X-ray analyzer (EDX). Infrared

S. E. Trolier-McKinstry—contributing editor

Manuscript No. 22784. Received February 8, 2007; approved July 19, 2007.
This work was financially supported by the Department of Science and Technology (DST), Government of India, New Delhi
[†]Author to whom correspondence should be addressed. e-mail: shiva@sscu.iisc.ernet.in

spectra for calcined samples were recorded on a Perkin-Elmer (Germany) FT-IR Spectrometer spectrum 1000 from 300 to 4000 cm^1. Electrical resistivity measurement was carried out on the sintered pellets at 800°C for 12 h by a four-probe method in the temperature range from 300 to 12 K. Room temperature magnetic measurements were carried out using a vibrating sample magnetometer (VSM; Lake Shore).

(1) Determination of Mn^{3+}/Mn^{4+} Concentration

The ratio of the Mn^{3+}/Mn^{4+} concentration was determined by iodometric titration for the sintered compounds.[9] Typically, about 50 mg of the compound was dissolved in 10 mL of 1:1 HCl containing about 1 g of solid KI. Liberated iodine was titrated against standard sodium thiosulphate (0.05 N) solution using starch as an indicator.

(2) Determination of Sodium Content

Sodium content was estimated by flame photometry. About 50 mg of the compound was dissolved in 10 mL of 6*M* HCl, evaporated to dryness, and redissolved in 100 mL of deionized water. Standard solutions were prepared from analytical grade (AR) NaCl salts dried at 200°C. The accuracy of estimation is within ± 0.02.

III. Results and Discussions

Figure 1 shows the powder XRD patterns for the typical $La_{0.85}Na_{0.15}MnO_3$ (a) as synthesized and sintered at 800°C from 5 min to 2 h (Figs. 1(b)–(g)). The as-synthesized compound is amorphous in nature. However the fact that a crystalline perovskite oxide is formed within 5 min of sintering at 800°C shows that the amorphous product contains the metal oxides, probably in the nanoparticulate form. The question arises as to why the as-synthesized product is amorphous in this system. In this system, it is necessary to moderate the flame temperature in order to suppress the loss of sodium ions at the cost of crystallinity. The exothermicity of the combustion reaction depends on the oxidizer (O) to fuel (F) ratio and the maximum is observed when O/F = 1. Here, we have controlled the exothermicity of the reaction by making it fuel lean, i.e., by adding excess nitrate source (Oxidizer). As a result of less exothermic reaction, the products formed are amorphous and the composition is nearer to nominal as the Na ion evaporation is fully controlled. The XRD pattern in the product oxide could be indexed in rhombohedral symmetry having the lattice parameters $a = 5.495(8)$ Å and $c = 13.354(4)$ Å (hexagonal setting) with space group *R*-3*c* (No. 167). There is no structural change with increasing sintering time. The average crystallite size from XRD data was calculated using the Debye–Scherrer formula[19] and the crystallite size increases with increasing sintering time. Increase in crystallite size is not significant after 1 h heating at 800°C. The crystallite sizes were found to be in the range of 25–34 nm. We also studied the growth of particle size in the $La_{0.85}Na_{0.15}MnO_3$ system with temperature. The compound was heated in the temperature range from 500° to 800°C at a fixed duration of an hour, single-crystalline phase was observed at 500°C itself. The compound crystallized in the rhombohedral structure with space group *R*-3*c* (No.167). Here also, there is no structural change with increasing temperature from 500° to 800°C, the crystallite size increases with increasing temperature up to 800°C. The average crystallite sizes were in the range of 21–33 nm.

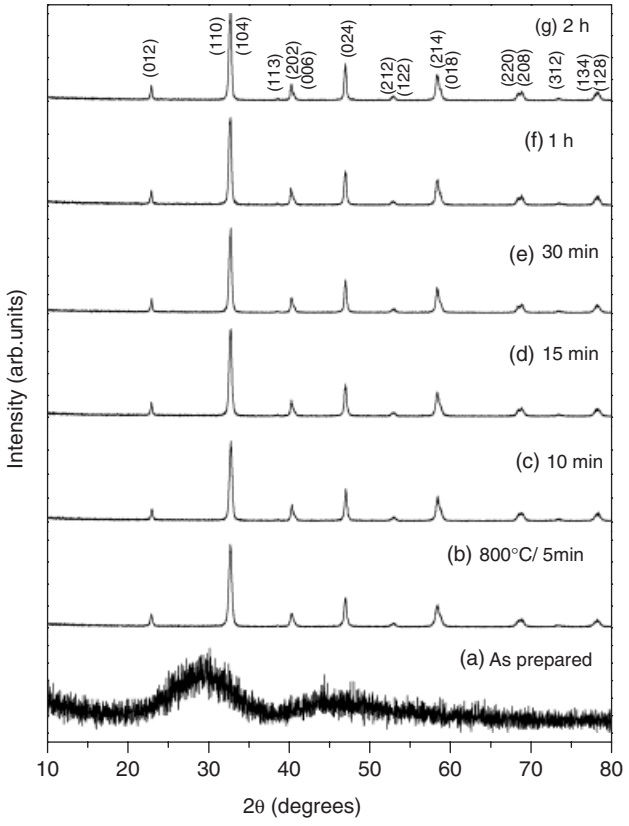

Fig. 1. Powder X-ray diffraction patterns of $La_{0.85}Na_{0.15}MnO_{2.937}$ compound sintered at 800°C from 5 min to 2 h.

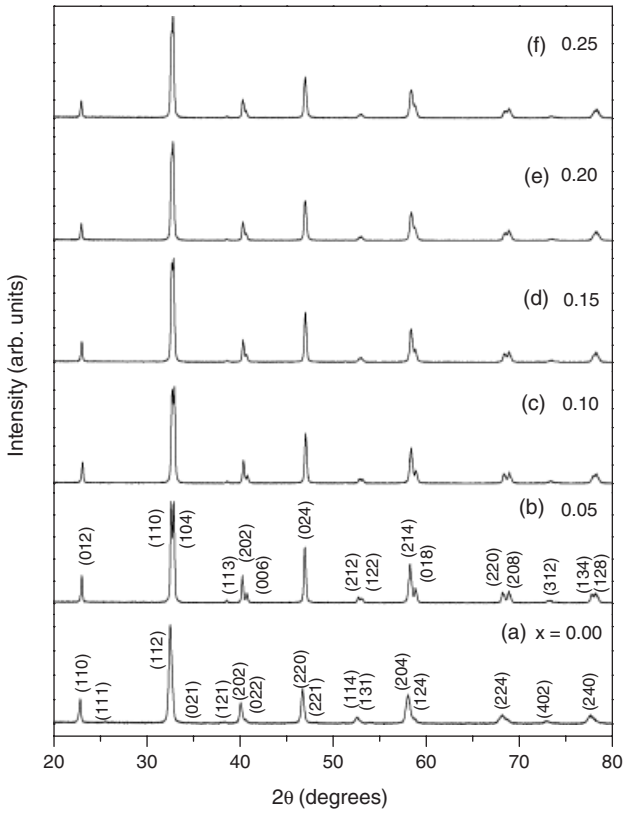

Fig. 2. Powder X-ray diffraction patterns of $La_{1-x}Na_xMnO_3$ ($0.00 \le x \le 0.25$) phases, sintered at 800°C/2 h.

We synthesized a series of sodium-substituted lanthanum manganites having the general formula, $La_{1-x}Na_xMnO_3$ ($0.00 \le x \le 0.25$), as aliovalent doping of La^{3+} by Na^+ is expected to generate twice the Mn^{4+} content when compared with the better-known Sr^{2+}-doped system.[16] As-prepared samples were heated at 800°C for 2 h. In Fig. 2, we have shown the powder XRD patterns of all the compounds. The parent $LaMnO_3$ compound crystallizes in the orthorhombic structure with space group *Pbnm* (No. 62), and the indexed diffraction pattern is shown in Fig. 2(a). The sodium-substituted compounds crystallize in the rhombohedral structure (hexagonal setting) with space group *R*-3*c* (No.167), indexed powder XRD pattern is

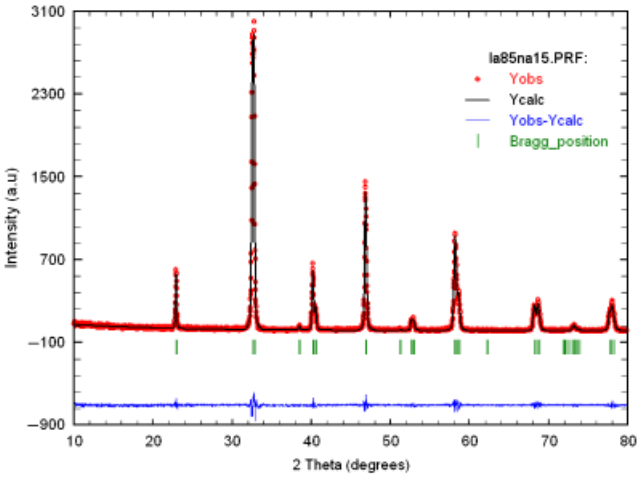

Fig. 3. Typical, observed, calculated, and the difference Rietveld refined X-ray diffraction pattern of $La_{0.85}Na_{0.15}MnO_{2.937}$ compound.

given for the composition $La_{0.95}Na_{0.05}MnO_3$ in Fig. 2(b). As the sodium content increased from $x = 0.05$ to 0.25, the rhombohedral phase transfers to cubic-like symmetry Fig. 2(b–f). The splitting of the main (110) and (104) lines decreases and seems to merge into one line with increasing Na content. The structural parameters for all the phases were obtained from the Rietveld refinement method. The refinement results reveals that even 25% sodium content also crystallizes in the rhombhohedral structure with less rhombohedral distortion. In Fig. 3, observed, calculated, and the difference XRD pattern of the typical $La_{0.85}Na_{0.15}MnO_{2.937}$ is given. There is good agreement between the observed and calculated patterns. In Table I, we have summarized refined structural parameters, Mn–O bond lengths, and Mn–O–Mn bond angles for all the samples. In Fig. 4, we have shown the plot of (a) unit cell volume per formula unit and (b) Mn–O–Mn bond angle as a function of sodium content. When sodium content increases from $x = 0.05$ to 0.25, the unit cell volume decreases from 58.52 to 57.98 (Å^3) and Mn–O–Mn bond angle increases from 164.16 to 166.39°. The decrease in cell volume can be correlated with the increase in Mn^{4+} content, which is smaller (ionic radii, 0.53 Å) than the Mn^{3+} ion (ionic radii, 0.645 Å). The presence of smaller cations in the B sub-lattice of the ABO_3 perovskite is responsible for both the reduction in unit cell volume and for the increase in the Goldschmidt tolerance factor ($t = d_{A\text{-}O}/\sqrt{2}d_{B\text{–}O}$), hence the decrease of the rhombohedral distortion of the lattice.[20]

The increase in Mn–O–Mn bond angle is explained based on the tolerance factor, t, of the system. In the perovskite system size, when A-site cation is large the tolerance factor, t, approaches 1. There is no distortion in the Mn–O–Mn bond angle, the structure is cubic. The parent oxide, $LaMnO_3$, crystallizes in the orthorhombic structure; the coordination number of La- ion is 9, the ionic radii of lanthanum ($r_{La3+} = 1.24$ Å). The Na-substituted compound crystallizes in the rhombohedral structure in which lanthanum and sodium ions have a 12 coordination ($r_{La3+} = 1.36$ Å; $r_{Na+} = 1.39$ Å) having three types of La/Na–O distances.[9] On increasing Na content, the crystal structure transforms to cubic-like symmetry. We did not see any splitting in the main line, but Rietveld refinement data reveal the

Table I. Rietveld Refined Structural Parameters, Selected Bond Angles, and Bond Lengths of $La_{1-x}Na_xMnO_3$ Samples

Compounds	$LaMnO_{3.075}$	$La_{0.95}Na_{0.045}MnO_{3.073}$	$La_{0.90}Na_{0.10}MnO_{3.045}$	$La_{0.85}Na_{0.15}MnO_{2.937}$	$La_{0.80}Na_{0.19}MnO_{2.983}$	$La_{0.75}Na_{0.23}MnO_{2.95}$
Crystal system	Orthorhombic	Rhombohedral	Rhombohedral	Rhombohedral	Rhombohedral	Rhombohedral
space group	*Pbnm* (62)	*R*-3*c* (167)	*R*-3*c* (167)	*R*-3*c* (167)	*R*-3*c* (167)	*R*-3*c* (167)
Lattice parameters						
a (Å)	5.477(6)	5.513(4)	5.509(4)	5.498(4)	5.489(5)	5.489(3)
b (Å)	5.524(4)					
c (Å)	7.805(6)	13.350(3)	13.341(5)	13.341(5)	13.329(2)	13.328(5)
Cell volume/formula unit (Å^3)	59.05	58.52	58.48	58.20	57.97	57.98
La/Na	(4e)	(6a)	(6a)	(6a)	(6a)	(6a)
x	0.005 (12)	0.0000	0.0000	0.0000	0.0000	0.0000
y	0.0120 (5)	0.0000	0.0000	0.0000	0.0000	0.0000
z	0.2500	0.2500	0.2500	0.2500	0.2500	0.2500
Mn	(4b)	(6b)	(6b)	(6b)	(6b)	(6b)
x	0.5000	0.0000	0.0000	0.0000	0.0000	0.0000
y	0.0000	0.0000	0.0000	0.0000	0.0000	0.0000
z	0.0000	0.0000	0.0000	0.0000	0.0000	0.0000
O1	(4e)	(18e)	(18e)	(18e)	(18e)	(18e)
x	0.0109 (7)	0.451 (3)	0.452 (4)	0.455 (6)	0.458 (5)	0.457(4)
y	0.4869 (6)	0.0000	0.0000	0.0000	0.0000	0.0000
z	0.2500	0.2500	0.2500	0.2500	0.2500	0.2500
O2	(8d)					
x	0.7500 (8)					
y	0.2803 (6)					
z	0.0675 (3)					
R-factors						
R_P	12.3	6.93	7.23	6.81	7.17	7.47
R_{WP}	18.0	11.40	11.90	11.00	12.2	11.8
R_{Bragg}	4.80	1.80	2.07	1.54	1.64	1.70
R_F	4.61	1.39	1.78	1.61	1.78	1.94
Bond lengths and angles						
Mn–O1–Mn (deg.)	174.49 (5)	164.16 (1)	164.47 (5)	165.45 (3)	166.41 (2)	166.09(3)
Mn–O2–Mn (deg.)	148.86 (8)					
Mn–O1 (Å)	1.953 (7)	1.960 (5)	1.958 (3)	1.953 (5)	1.948 (5)	1.949(4)
Mn–O2 (Å)	2.133 (2)					
Mn–O2′ (Å)	1.904 (2)					

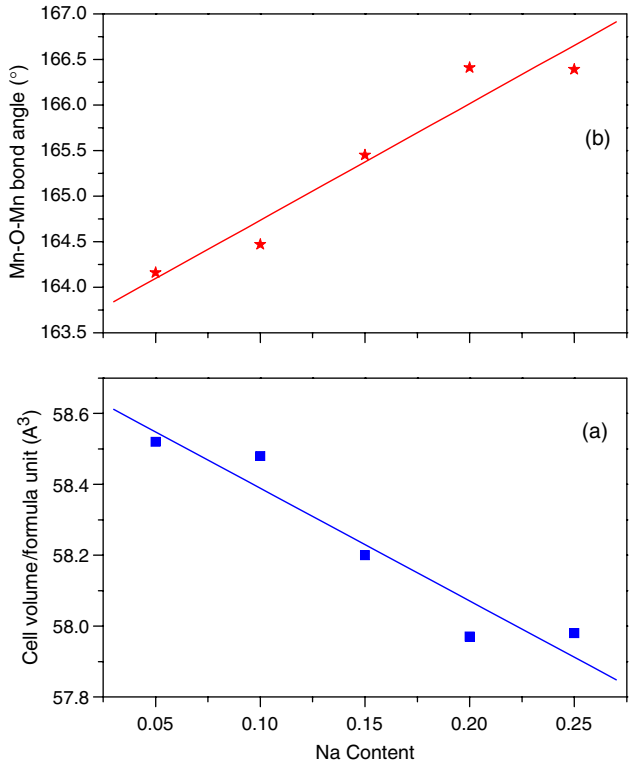

Fig. 4. Plots of (a) unit cell volume per formula unit and (b) Mn–O–Mn bond angle as a function of Na content.

structure to be rhombohedral symmetry with minor distortion. This implies that the Mn–O–Mn bond angle increases. A similar increase in bond angle in the perovskite system is reported in the literature[21] and sodium-doped lanthanum manganite by Roy *et al.*[22]

Wet chemical analysis results reveal that Mn^{4+} content increases with increasing sodium content from 15% to 42%. Parent $LaMnO_3$ compound showed minimum 15% of Mn^{4+} content, whereas 5%, 10%, 15%, 20%, and 25% sodium-substituted compounds showed 25%, 29%, 31%, 38%, and 42% of Mn^{4+} content, respectively. Contrary to expectations the compositions with a low x value are relatively richer in Mn^{4+}, and compositions with higher x values are relatively poorer than what is expected form the Na content. It may be recalled that it is difficult to make stoichiometric $LaMnO_3$ as some of the Mn is oxidized to 4+. The Na content was not only determined experimentally but also obtained by the refinement of the SOF during Rietveld refinement. Based on these measurements, final formula has been given for each composition (Table I).

Scanning electron micrographs of $La_{0.95}Na_{0.045}MnO_{3.075}$ (a) as-synthesized, (b) calcined powder for 2 h, and (c) sintered pellets at 800°C for 12 h are shown in Fig. 5. The micrograph of the as-synthesized sample shows voluminous and porous morphology. On calcination the growth in particle size and grain boundary is evident. The particles were agglomerated and the particle sizes are in the range of 2–5 μm. It is seen from Fig. 5(c) that the SEM image of sintered pellet shows high densification and compactability. EDX on the spot mode and overall area results reveal that compositions are homogeneous.

FT-IR spectra of $La_{1-x}Na_xMnO_3$ ($0.00 \le x \le 0.25$) compounds are shown in Figs. 6(a)–(f). The IR spectrum shows two absorption bands around 600 and 400 cm^{-1} for the compositions (a) $x = 0.0$, (b) 0.05, and (c) 0.10. The higher frequency band at 600 cm^{-1} was assigned to the Mn–O stretching vibration mode, which involves the internal motion of a change in Mn–O bond length, the band around 400 cm^{-1} corresponds to the bending mode, which is sensitive to a change in the Mn–O–Mn bond angle. These two bands are related to the environment surrounding the MnO_6 octahedra in the ABO_3 perovskite.[23,24]

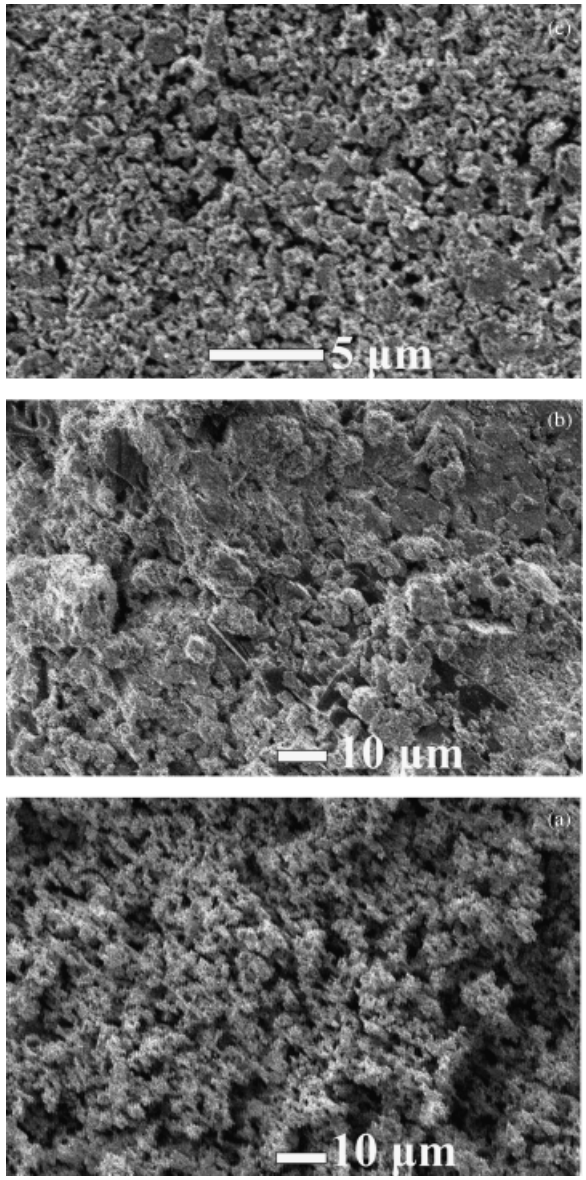

Fig. 5. Scanning electron micrographs of $La_{0.95}Na_{0.045}MnO_{3.073}$ (a) as-synthesized, (b) calcined powder at 800°C for 2 h, and (c) sintered pellets at 800°C for 12 h.

These absorptions disappear when x exceeds 0.15, on account of the metallic nature of the oxides (Figs. 6(d)–(f)).

In Fig. 7, we have shown the resistivity as a function of temperature plots of $La_{1-x}Na_xMnO_3$ ($0.00 \le x \le 0.25$) samples. The composition $x = 0.00$ exhibits insulating behavior. Increase in sodium content from $x = 0.05$ to 0.25 reveals a composition-controlled metal to insulator transition (T_{M-I}). The T_{M-I} values observed in the present study were 145, 215, 280, 230, and 225 K for the compositions $x = 0.05$, 0.10, 0.15, 0.20, and 0.25, respectively. Generally, solid-state preparations yield a bigger grain size and exhibit sharp metal insulator transitions. However in the present study, all the samples show a broad metal insulator transition, which can be attributed to the nanocrystalline nature of the grains and the weak grain boundary contact. The effect of grain size on the magnetic, transport, and structural properties of manganites has been extensively studied by many investigators.[25–28] These studies suggest that particle size, the doping level in the lanthanum site as well as oxygen content play an important role in the above properties of these class of oxides. Here $x = 0.20$ and 0.25 compositions exhibit low values of T_{M-I} 230 and 225 K, because of these compounds having high Mn^{4+} content of 38% and 42%, respectively.

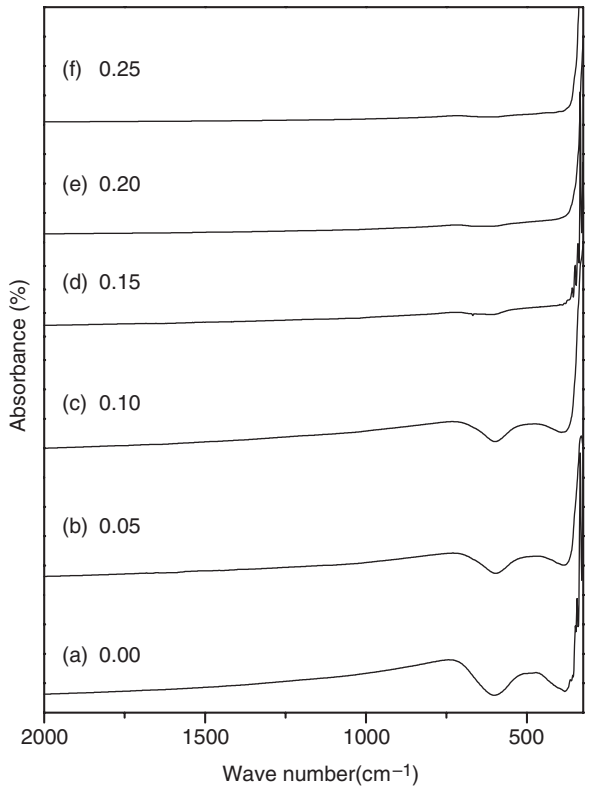

Fig. 6. Fourier transform infrared spectra of $La_{1-x}Na_xMnO_3$ ($0.00 \leq x \leq 0.25$) phases for sintered samples at 800°C for 2 h.

Growth of the particle size as a function of time and temperature was correlated with magnetic properties. In Figs. 8(a)–(g), we have shown the change in magnetic moment as a function of applied field for $La_{0.85}Na_{0.15}MnO_{2.937}$ sintered at 800°C for

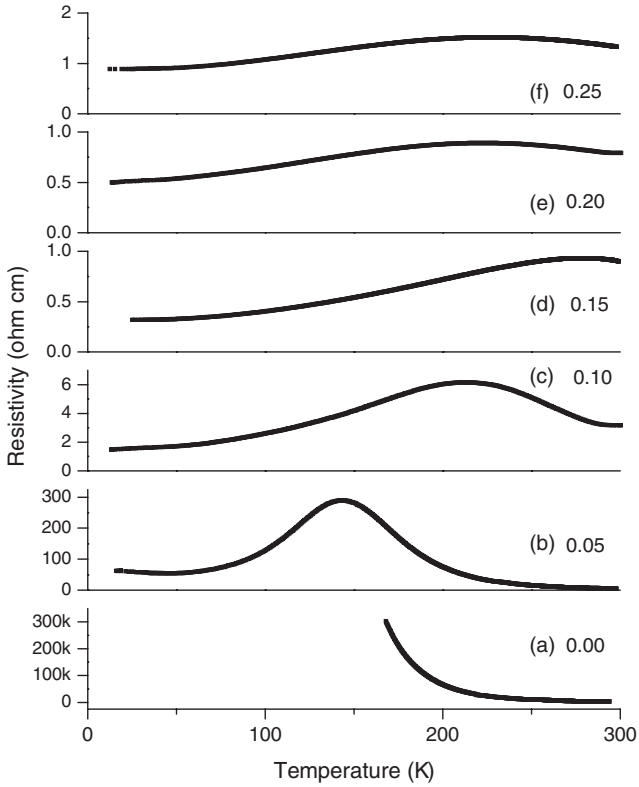

Fig. 7. Plots of electrical resistivity as a function of temperature for $La_{1-x}Na_xMnO_3$ ($0.00 \leq x \leq 0.25$) compounds sintered at 800°C for 12 h.

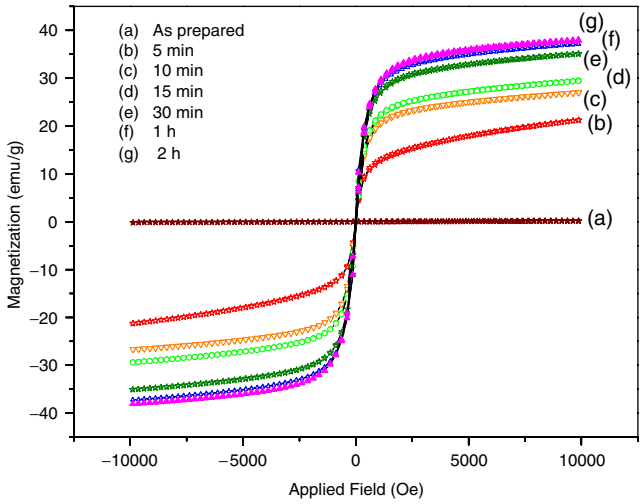

Fig. 8. Magnetization as a function of applied field for $La_{0.85}Na_{0.15}MnO_{2.937}$ compound sintered at 800°C for different time.

different times from 5 min to 2 h. In the present work, the as-synthesized sample is not a perovskite phase, therefore we did not see any ferromagnetism in the sample. On increasing the sintering time from 5 min to 2 h, the magnetic moment increased concomitantly with the increase in crystallite size. In Fig. 9(a), we have shown the sintering time versus crystallite size and magnetic moment for the $La_{0.85}Na_{0.15}MnO_{2.937}$ compound. As can be seen from the plots, the compound heated for 60 min

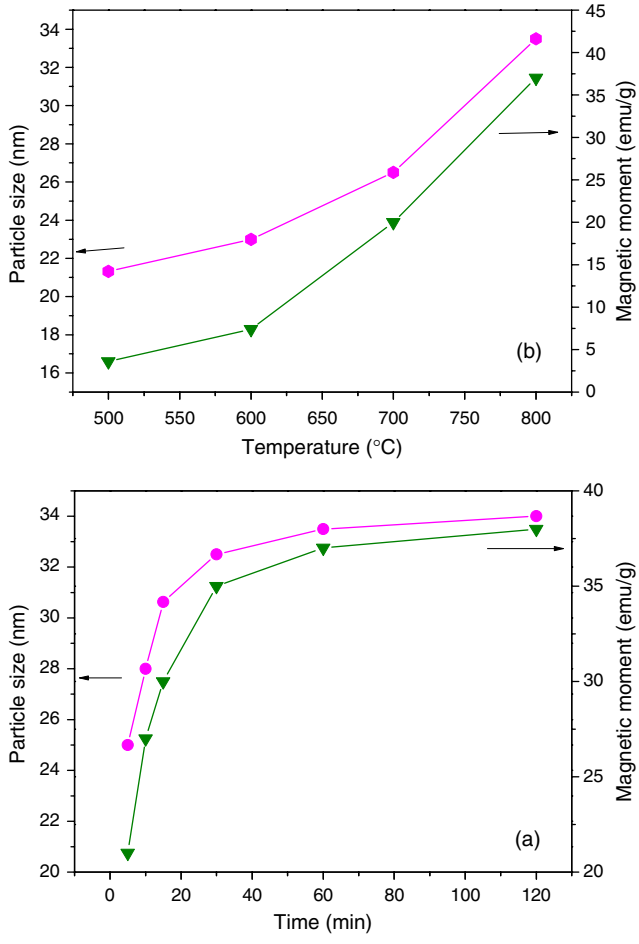

Fig. 9. Plots of (a) sintering time (800°C) versus crystallite size and magnetic moment for $La_{0.85}Na_{0.15}MnO_{2.937}$ (b) Sintered temperature (time, 1 h) versus crystallite size and magnetic moment for $La_{0.85}Na_{0.15}MnO_{2.937}$ compound.

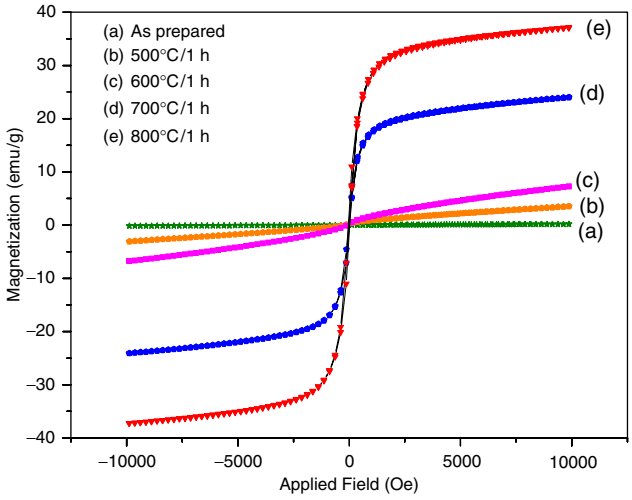

Fig. 10. Plots of magnetization as a function of applied field for $La_{0.85}Na_{0.15}MnO_{2.937}$ samples sintered at temperature from 500° to 800°C for 1h.

showed 36 emu/g and increase in magnetic moment was not significant when sintered further.

Similarly, we performed the magnetization measurement for $La_{0.85}Na_{0.15}MnO_{2.937}$ sintered at different temperatures from 500° to 800°C for a fixed duration of 1 h, as shown in Figs. 10(a)–(e). From Fig. 10, it is clear that samples heated up to 600°C for 1 h did not show any magnetic saturation up to 10 K Oe, whereas 700°- and 800°C-sintered samples did show magnetic saturation. This indicates compounds crystallized in the perovskite phase at as low as 500°C, in order to get ferromagnetic ordering we have to heat the sample at a minimum temperature of 700°C for 1 h. Sintering temperature as a function of magnetic moment and crystallite size is shown in Fig. 9(b). This shows an increase in magnetic moment as well as in crystallite size with increase in sintering temperature and time. Figures. 9(a) and (b) clearly demonstrates that particle size plays an important role in magnetic ordering rather than structural order.

Figure 11 shows the magnetization versus applied field for all the phases of $La_{1-x}Na_xMnO_3$ ($0.00 \le x \le 0.25$) sintered at 800°C for 2 h. For the compositions (a) 0.00, (b) 0.05, and (c) 0.10 exhibit paramagnetic behavior with the magnetic moment of 0.6, 1.2, and 7.0 emu/g, respectively. On the other hand, as the sodium content increases from (d) 0.15, (e) 0.20 and (f) 0.25

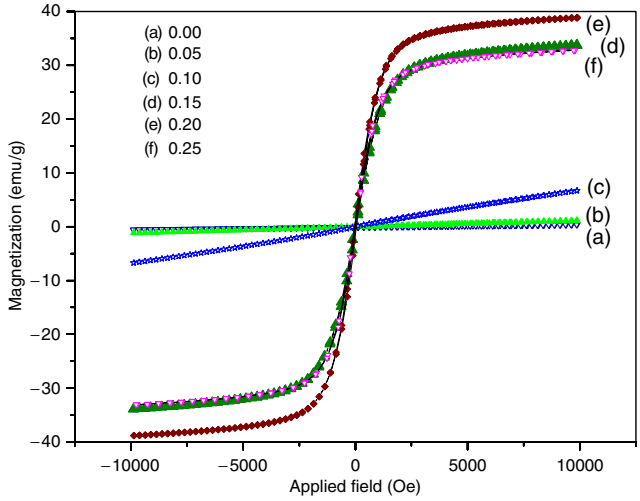

Fig. 11. Magnetization as a function of applied field for $La_{1-x}Na_xMnO_3$ ($0.00 \le x \le 0.25$) compounds sintered at 800°C for 2 h.

compounds are ferromagnetic with magnetic moments 34, 39, and 33 emu/g, respectively. Magnetic moment of the $La_{0.75}Na_{0.23}MnO_{2.95}$ phase is lower than that of $La_{0.80}Na_{0.19}MnO_{2.983}$. This is because, Mn^{4+} content is 42% in $La_{0.75}Na_{0.23}MnO_{2.95}$ system, which favors antiferromagnetic interaction within the ferromagnetic clusters.[29] Washburn *et al.*[30] have analyzed such a magnetic behavior taking into account two lattice models, one with ferromagnetic interaction and the other with antiferromagnetic interaction. Here, in addition to $Mn^{3+}-O-Mn^{4+}$ double-exchange interaction leading to ferromagnetic behavior, $Mn^{4+}-O-Mn^{4+}$ is antiferromagnetic interaction, which brings down the ferromagnetic interaction and hence the magnetic moment is lower in the $La_{0.75}Na_{0.23}MnO_{2.95}$ system.

IV. Conclusions

In conclusion, we have shown Na^+ ion substituted for La site in the $LaMnO_3$ system by the rapid solution combustion method and up to 25% of Na can be substituted for La by this method. Structural transition was observed from orthorhombic to rhombhohedral on substitution of sodium. We have observed the structural ordering temperature as low as 500°C as well as a shorter duration of 5 min at 800°C. Room temperature VSM data reveal that particle size plays an important role in magnetic ordering rather than the structural order.

Acknowledgments

Special thanks are due to Professor M. S. Hegde, SSCU, Indian Institute of Science for useful discussion and support.

References

[1]G. H. Jonker and J. H. Van Santen, "Ferromagnetic Compounds of Manganese With Perovskite Structure," *Physica*, **16** [3] 337–49 (1950).

[2]R. von Helmolt, J. Wecker, B. Holzapfel, L. Schultz, and K. Samwer, "Giant Negative Magnetoresistnace in Perovskite Like $La_{2/3}Ba_{1/3}$ MnO_x Ferromagnetic Films," *Phys. Rev. Lett.*, **71**, 2331–3 (1993).

[3]C. N. R. Rao, "Charge, Spin, and Orbital Ordering in the Perovskite Manganates, $Ln_{1-x}A_xMnO_3$ (Ln) Rare Earth, (A) Ca or Sr)," *J. Phys. Chem.*, **B104**, 5877–89 (2000).

[4]M. Itoh, T. Shimura, J. D. Yu, T. Hayashi, and Y. Inaguma, "Structure Dependence of the Ferromagnetic Transition Temperature in Rhombohedral $Ln_{1-x}A_xMnO_3$ (A = Na, K, Rb, and Sr)," *Phys. Rev.*, **B52**, 12522–5 (1995).

[5]T. Shimura, T. Hayashi, Y. Inaguma, and M. Itoh, "Magnetic and Electrical Properties of $La_yA_xMn_wO_3$ (*A* 5 Na, K, Rb, and Sr) With Perovskite-Type Structure," *J. Solid State Chem.*, **124**, 250–63 (1996).

[6]M. Sahana, R. N. Singh, C. Shivakumara, N. Y. Vasanthacharya, M. S. Hegde, S. Subramanian, V. Prasad, and S. V. Subramanyam, "Colossal Magnetoresistance in Epitaxial $La_{(12x2y)})Na_yMnO_3$ Thin Film," *Appl. Phys. Lett.*, **70**, 2909–11 (1997).

[7]C. C. Chen and A. de Lozanne, "Simultaneous Electronic and Magnetic Transitions in $La_{1-x}K_xMnO_3$ Thin Films," *Appl. Phys. Lett.*, **71**, 1424–6 (1997).

[8]Y. Ng-Lee, F. Safina, E. Martinez-Tamayo, J. V. Folgado, R. Ibanez, D. Beltran, F. Lloret, and A. Segura, "Low-Temperature Synthesis, Structure and Magnetoresistance of Submicrometric $La_{1x}K_xMnO_{3+d}$ Perovskites," *J. Mater. Chem.*, **7**, 1905–9 (1997).

[9]R. N. Singh, C. Shivakumara, N. Y. Vasanthacharya, S. Subramanian, M. S. Hegde, S. Rajagopal, and A. Sequeira, "Synthesis, Structure, and Properties of Sodium or Potassium-Doped Lanthanum Orthomanganites from NaCl or KCl Flux," *J. Solid State Chem.*, **137**, 19–27 (1998).

[10]W. H. McCarroll, Ian D. Fawcett, M. Greenblatt, and K. V. Ramanujachary, "Synthesis and Properties of Lanthanum Sodium Manganate Perovskites Crystals," *J. Solid State Chem.*, **146**, 88–95 (1999).

[11]K. C. Patil, S. T. Aruna, and S. Ekambaram, "Combustion Synthesis," *Curr. Opin. Solid State Mater. Sci.*, **2**, 158–65 (1997).

[12]P. Bera, K. C. Patil, and M. S. Hegde, "NO Reduction, CO and Hydrocarbon Oxidation Over Combustion Synthesized Ag/CeO_2 Catalyst," *Phys. Chem. Chem. Phys.*, **2**, 3715–9 (2000).

[13]P. Bera, S. T. Aruna, K. C. Patil, and M. S. Hegde, "Studies on Cu/CeO_2: A New NO Reduction Catalyst," *J. Catal.*, **186**, 36–44 (1999).

[14]S. T. Aruna, M. Muthuraman, and K. C. Patil, "Combustion Synthesis and Properties of Strontium Substituted Lanthanum Manganites $La_{1-x}Sr_xMnO_3$ ($0.0 \le x \le 0.3$)," *J. Mater. Chem.*, **7** [12] 2499–503 (1997).

[15]B. M. Nagabhushana, G. T. Chandrappa, R. P. Sreekanth Chakradhar, K. P. Ramesh, and C. Shivakumara, "Synthesis, Structural and Transport Properties of Nanocrystalline $La_{1x}Ba_xMnO_3$ ($0.0 \le x \le 0.3$) Powders," *Solid State Commun.*, **136** [7] 427–32 (2005).

[16]B. M. Nagabhushana, R. P. Sreekanth Chakradhar, K. P. Ramesh, C. Shivakumara, and G. T. Chandrappa, "Low Temperature Synthesis,

Structural Characterization, and Zero-Field Resistivity of Nanocrystalline $La_{1-x}Sr_xMnO_{3+\delta}$ ($0.0 \leq x \leq 0.3$) Manganites," *Mater. Res. Bull.*, **41** [9] 1735–46 (2006).

[17]L. Malavasi, M. C. Mozzati, S. Polizzi, C. B. Azzoni, and G. Flor, "Nanosized Sodium-Doped Lanthanum Manganites: Role of the Synthetic Route on their Physical Properties," *Chem. Mater.*, **15**, 5036–43 (2003).

[18]K. C. Patil, "Advanced Ceramics: Combustion Synthesis and Properties," *Bull. Mater. Sci.*, **16**, 533–41 (1993).

[19]P. Scherrer, "Determination of the Size and the Internal Structure of Colloid Particles by Means of X-ray," *Nachr. Ges. Wiss. Gottingen, Math.-Phys.*, **2**, 98–100 (1918).

[20]M. Yahia and H. Batis, "Properties of Undoped and Ca-Doped $LaMnO_3$—Non-Stoichiometry and Defect Structure," *Eur. J, Inorg. Chem.*, 2486–94 (2003).

[21]J. B. Torrance, P. Lacorre, A. I. Nazzal, E. J. Ansaldo, and ch. Niedermayer, "Systematic Study of Insulator–Metal Transitions in Perovskites $RNiO_3$ (R = Pr, Nd, Sm, Eu) Due to Closing of Charge Transfer Gap," *Phy. Rev. B*, **45** [14] 8209–12 (1992).

[22]S. Roy, Y. Q. Guo, S. Venkatesh, and N. Ali, "Interply of Structure and Transport Properties of Sodium-Doped Lanthanum Manganite," *J. Phys.: Condens. Matter.*, **13**, 9547–57 (2001).

[23]F. Gao, R. A. Lewis, X. L. Wang, and S. X. Dou, "Far-Infrared Reflection and Transmission of $La_{1x}Ca_xMnO_3$," *J. Alloys Compd.*, **347** [1–2] 314–8 (2002).

[24]A. Arulraj and C. N. R. Rao, "An Infrared Spectroscopic Study of the Insulator–Metal Transition and Charge-Ordering in Rare Earth Manganates, $Ln_{1x}A_xMnO_3$ (Ln = Rare Earth, A = Ca, Sr, Pb)," *J. Solid State Chem.*, **145** [2] 557–63 (1999).

[25]R. Mahendiran, R. Mahesh, A. K. Raychaudhuri, and C. N. R. Rao, "Resistivity, Giant Magnetoresistance and Thermopower in $La_{0.7}Sr_{0.3}MnO_3$ Showing a Large Difference in Temperatures Corresponding to the Ferromagnetic Transition and the Insulator—Metal Transition," *Solid State Commun.*, **99** [3] 149–52 (1996).

[26]J. Wang, B. Gu, H. Sang, G. Ni, and Y. Du, "Grain-Size Dependence of Complex Permeability in Polycrystalline Perovskite $La_{0.7}Sr_{0.3}MnO_3$," *J. Magn. Magn. Mater.*, **223** [1] 50–4 (2001).

[27]J. Yang, B. C. Zhao, R. L. Zhang, Y. Q. Ma, Z. G. Sheng, W. H. Song, and Y. P. Sun, "The Effect of Grain Size on Electrical Transport and Magnetic Properties of $La_{0.9}Te_{0.1}MnO_3$," *Solid State Commun.*, **132** [2] 83–7 (2004).

[28]L. E. Hueso, F. Rivadulla, R. D. Sanchez, D. Caeiro, C. Jardon, C. Vazquez–Vazquez, J. Rivas, and M. A. Lopez–Quintela, "Influence of the Grain-Size and Oxygen Stoichiometry on Magnetic and Transport Properties of Polycrystalline $La_{0.67}Ca_{0.33}MnO_{3\pm\delta}$ Perovskites," *J. Magn. Magn. Mater.*, **189** [3] 321–8 (1998).

[29]C. Shivakumara, G. N. Subbanna, N. P. Lalla, and M. S. Hegde, "Na-Substitution for La- and Mn-Sites in $LaMnO_3$ from Alkali Halide Fluxes: Low Temperature Synthesis, Structure and Properties," *Mater. Res. Bull.*, **39**, 71–81 (2004).

[30]N. R. Washburn and A. M. Stacy, "Magnetic and Transport Properties of $LaMn_{0.8}Na_{0.2}O_3$," *J. Phys. Chem. B*, **104**, 1447–53 (2000). □